Journal of Catalysis 261 (2009) 158–165

Contents lists available at ScienceDirect

Journal of Catalysis

www.elsevier.com/locate/jcat

Effect of boron on the stability of Ni catalysts during steam methane reforming

Jing Xu [a], Luwei Chen [b], Kong Fei Tan [a], Armando Borgna [b,*], Mark Saeys [a,*]

[a] Department of Chemical and Biomolecular Engineering, 4 Engineering Drive 4, National University of Singapore, Singapore 117576, Singapore
[b] Institute of Chemical and Engineering Sciences, A*STAR (Agency for Science, Technology and Research), 1 Pesek Road, Jurong Island, Singapore 627833, Singapore

ARTICLE INFO

Article history:
Received 25 July 2008
Revised 25 October 2008
Accepted 8 November 2008
Available online 9 December 2008

Keywords:
Boron
Ni catalyst
Steam reforming
Carbon deposition
Catalyst deactivation

ABSTRACT

Ni catalysts promoted with 0.5 and 1.0 wt% boron were synthesized, characterized and tested during steam methane reforming, to evaluate the effect of boron on the deactivation behavior. Boron adsorbs on the γ-Al_2O_3 support and on the Ni particles and 1.0 wt% boron is found to enhance the stability without compromising the activity. Catalytic studies at 800 °C, 1 atm, a stoichiometric methane to steam ratio, and space velocities of 330,000 $cm^3/(h\,g_{cat})$ show that promotion with 1.0 wt% boron reduces the rate of deactivation by a factor of 3 and increases the initial methane conversion from 56% for the unpromoted catalyst to 61%. Temperature-programmed oxidation (TPO) and scanning electron microscopy (SEM) studies confirm the formation of carbonaceous deposits and illustrate that 1.0 wt% boron reduces the amount of deposited carbon by 80%.

1. Introduction

Steam reforming of hydrocarbons is the dominant process for the industrial scale production of hydrogen [1,2]. As the demand for hydrogen is increasing, this process is likely to further gain importance. Steam reforming converts hydrocarbons, in particular methane, and steam into syngas, a mixture of CO and H_2. Ni is the dominant commercial catalyst because of its good catalytic activity and its cost-effectiveness as compared to Pt, Ru or Rh-based catalysts. However, carbon deposition, so-called coking, is especially severe for Ni-based catalysts and leads to rapid catalyst deactivation [3]. Enhancing the stability of Ni-based catalysts has therefore been an area of intensive research [4–9], and various promoters have been proposed. One of the oldest proposals is to introduce trace amount (2 ppm) of H_2S with the feed gas [4]. This method is industrially implemented in the Sulfur Passivated Reforming (SPARG) Process and was developed by Rostrup–Nielsen [4]. Sulfur selectively poisons the most active sites of the Ni catalyst, believed to be the step sites, leading to a small loss in the reforming activity. However, trace amounts of sulfur affect the deactivation rate much more than the reforming rate [5]. More recently, promoters such as Au [6,7], K [1,8], and Sn [9] have been proposed and shown to improve the stability of Ni catalysts.

A number of recent first principles studies of carbon chemisorption on Ni surfaces have further refined the molecular level understanding of the behavior of carbon atoms on a Ni catalyst [7,10]. These studies are briefly summarized in Section 2. Based on first principles calculations, we propose that small amount of boron could possibly enhance the stability of Ni catalysts [10]. Since boron and carbon exhibit similar chemisorption preferences on Ni catalysts, small amount of boron might selectively block the most stable binding sites. Calculations indicate that those sites might initiate coke formation [7,10] or lead to a loss in catalytic activity when occupied by carbon atoms [11]. Blocking them first by boron therefore potentially reduces deactivation.

In Section 4, we present experimental studies of the effect of boron on the stability of a Ni catalyst during steam methane reforming. Supported Ni catalysts were synthesized and promoted with 0.5 and 1.0 wt% boron, characterized using X-ray diffraction (XRD), H_2 temperature-programmed desorption (TPD), and X-ray photoelectron spectroscopy (XPS), and tested in a fixed-bed microreactor. The catalytic studies demonstrate that promotion with 1.0 wt% boron significantly reduces the deactivation rate. In addition, boron is found to enhance the initial methane conversion. These findings are consistent with first principles based predictions.

2. Coking mechanism on Ni catalysts and effect of promoters

In this section we briefly summarize studies of the coking mechanism on Ni catalysts, and discuss how different promoters are believed to affect catalyst stability. Surface carbon atoms are generally accepted as key reaction intermediates in the conversion of hydrocarbons to syngas [7], though recently an alternative mechanism via CHO was proposed for the catalytic partial oxidation of methane over Rh(111) [12]. Surface carbon atoms then react

* Corresponding authors. Faxes: +65 6316 6182, +65 6779 1936.
E-mail addresses: Armando_Borgna@ices.a-star.edu.sg (A. Borgna), chesm@nus.edu.sg (M. Saeys).

0021-9517/$ – see front matter
doi:10.1016/j.jcat.2008.11.007

Table 1
Calculated binding energies (kJ/mol) for carbon and boron atoms on Ni surfaces.[a]

Site	Carbon	Boron
On-surface hcp[b]	−662	−572
Subsurface octahedral	−707[b], −611[c]	−620[b], −648[c]
Bulk octahedral[d]	−686	−570
Step 5-fold hollow[e]	−752	−672
Graphene	−760	

[a] Details about the DFT calculations can be found in [10,11].
[b] Ni(111)-p(2 × 2) unit cell.
[c] 100% C/B in subsurface sites.
[d] C/B:Ni ratio = 1:8.
[e] Ni(211)-(1 × 2) unit cell.

with surface oxygen atoms to form CO. However, surface carbon atoms can also diffuse to subsurface octahedral sites or combine with other surface carbon atoms to ultimately form graphene islands. Carbon binding energies for different forms of deposited carbon are summarized in Table 1. Extended graphene islands are the most stable form of carbon on a Ni catalyst, with a carbon binding energy of −760 kJ/mol. On-surface carbon atoms are relatively unstable with binding energies of around −660 kJ/mol. Hence, the thermodynamic driving force to form graphene is significant. Graphene formation is generally unwanted, as graphene sheets cover active sites and hence lead to a loss in activity. However, the formation of graphene islands resembles a crystallization process and small islands are thermodynamically unstable [7,10]. Steps provide the most stable adsorption sites for carbon atoms (Table 1) and have been proposed as nucleation sites for the formation of graphene islands [7]. Promoters such as S, K, and Au preferentially bind to the step sites [7] and hence delay graphene formation and catalyst deactivation [4,6].

Subsurface octahedral sites are also preferred over on-surface sites [10] (Table 1), and subsurface carbon easily builds up under typical reaction conditions [13]. The presence of subsurface carbon significantly increases the calculated methane activation energy for a Ni(111) surface from 91 to 143 kJ/mol [11], and hence might reduce the catalyst activity. Boron and carbon atoms show a similar relative binding preference (Table 1), and boron is proposed to selectively block both step and subsurface sites [10,11]. Calculations indicate that boron atoms preferentially bind to step sites and to octahedral sites just below the surface [11] (Table 1), and hence might prevent the build-up of deposited carbon. Interestingly, subsurface boron becomes more stable at higher concentrations. This effect can be attributed to attractive interactions between boron atoms in neighboring octahedral sites. Subsurface boron also has a significant effect on the surface structure of the Ni catalyst. The boron–boron interactions cause a surface reconstruction where one row of Ni atoms moves up by 0.27 Å, while the other moves down by 0.31 Å (Fig. 1), and the reconstructed surface begins to resemble a stepped surface. This reconstruction lowers the surface energy by 0.38 J/m^2. To evaluate the effect of subsurface boron and of the surface reconstruction on the activity of the Ni catalyst, methane activation barriers were calculated for the terrace sites [11]. Methane activation has been proposed as the rate determining step for methane steam reforming over unpromoted Ni catalysts [14]. If subsurface boron has an effect similar to subsurface carbon and increases the methane activation barrier, then the catalyst activity might decrease by boron promotion. However, the activity does not necessarily increase if the barrier decreases, since other steps in the mechanism might become rate controlling. Fortunately, Density Functional Theory (DFT) calculations indicate that the surface reconstruction caused by subsurface boron significantly reduces the methane activation barrier from 91 kJ/mol on the Ni(111) surface to 64 kJ/mol [11] (Fig. 1). Hence, boron promotion is proposed to enhance the catalyst stability, without reducing the activity.

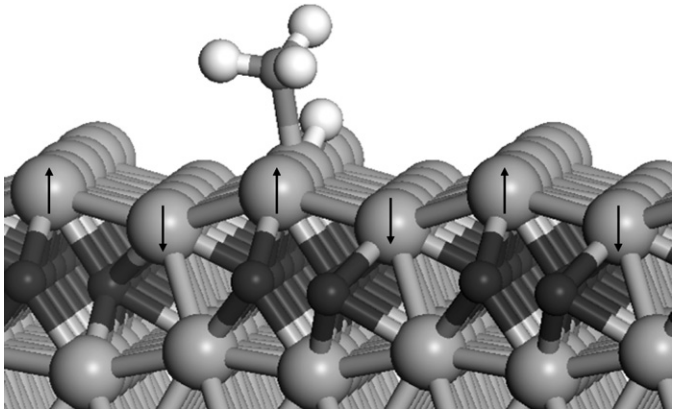

Fig. 1. Transition state structure for methane activation on the reconstructed Ni(111) surface promoted with subsurface boron. Small black, gray and white balls indicate boron, carbon and hydrogen atoms, respectively, while large gray balls correspond to Ni atoms. Arrows indicate the surface reconstruction.

Based on first principles calculations, Nikolla et al. [9] recently proposed Sn as a promoter to enhance the stability of Ni catalysts. Sn forms a surface alloy with Ni, and DFT calculations indicate that the presence of surface Sn atoms increases the C and O surface diffusion barriers. Sn is calculated to affect the selectivity between C–O and C–C bond formation, and the overall rate of C-oxidation is found to be much higher than that of C–C bond formation on a SnNi alloy catalyst. Experimental studies indeed confirm that small amounts of Sn (1.0 wt%) significantly reduce coke formation during methane and isooctane steam reforming at 800 °C, and for steam-to-carbon ratios between 0.5 and 1.5. Small amounts of Au also form a surface alloy with Ni [7,15]. DFT calculations [6] indicate that surface Au atoms significantly reduce the surface carbon binding energy at the neighboring Ni sites and the lower binding energy is suggested to lower the tendency to form a graphene overlayer [6]. In addition, recent DFT calculations indicate that Au atoms bind preferentially at the step sites [7] and might selectively block nucleation sites for graphene formation. The effect of 0.3 wt% Au on the stability of a 16.5 wt% Ni catalyst was demonstrated experimentally for butane reforming [6] at a space velocity of 1.2 h^{-1} and at 550 °C. A recent experimental study by Chin et al. [16] of the effect of promotion with Au on the structure, reactivity and stability of Ni catalysts during hydrocarbon steam reforming showed that small amounts of Au reduce carbon deposition during *n*-butane steam reforming between 450 and 550 °C. However, the effect of Au decreases with increasing temperatures and promotion with 0.4 wt% Au was found to decrease the initial methane conversion from 8.5 to 6.4% at 550 °C and for a steam-to-carbon ratio of 1.

3. Experimental details

3.1. Catalyst synthesis

Supported nickel catalysts were prepared by aqueous slurry impregnation using a nickel nitrate solution ($Ni(NO_3)_2{\cdot}6H_2O$, Acros Organics, 99% purity) to produce Ni loadings of approximately 15 wt% on a commercial γ-Al_2O_3 support with a surface area of 380 m^2/g (Pore volume: 0.87 ml/g). Following impregnation, the slurry was dried at 80 °C in a rotor evaporator, kept overnight at 80 °C in an oven, heated to 400 °C with a 1 °C/min ramp rate, and calcined in air at 400 °C for 2 h. After calcination, boric acid (H_3BO_3, Sigma–Aldrich, 99% purity) was sequentially introduced following the same preparation procedure to produce boron loadings of approximately 0.5 and 1.0 wt%.

The Ni and B loadings of the calcined catalysts were confirmed by inductively coupled plasma-optical emission spectrometry (ICP-

OES). The measured Ni:B atomic ratios for catalysts with 0.5 and 1.0 wt% B are identical to the theoretical ratios of 85:15 and 73:27, respectively.

3.2. Catalyst characterization

3.2.1. XRD

XRD was used to study the crystallographic structure of the calcined catalysts and performed on a Bruker D8 diffractometer using Cu$K\alpha$ radiation ($\lambda = 1.54$ Å). NiO and γ-Al_2O_3 phases were identified by comparison with database spectra. The average size of the NiO particles was estimated from the most intense NiO line at $2\theta = 43.3°$ using Scherrer's formula [17]. The NiO particle sizes, d(NiO), were converted to the corresponding Ni particle sizes after reduction, $d(Ni^0)$, using the relative molar volumes of metallic Ni and NiO [18]:

$$d(Ni^0) = 0.84d(NiO). \quad (1)$$

The dispersion D is then calculated from the average particle diameter, assuming spherical particles [19]:

$$D\ (\%) = \frac{90\ \text{nm}}{d(Ni^0)}. \quad (2)$$

Note that complete reduction of the calcined catalysts is assumed in the calculation. Experimental studies by Wei and Iglesia [14] however indicate that only between 30 and 50% of the NiO can be reduced following a similar procedure, and hence the number of active sites estimated from the XRD data for the calcined catalysts is likely an overestimation.

3.2.2. H_2 TPD

H_2 TPD was used to characterize the effect of B promotion on the surface active sites. 100 mg of catalyst was loaded into a pyrex tube, heated from room temperature to 120 °C at 5 °C/min and held at that temperature for 1 h under Ar. Next, catalysts were reduced in pure hydrogen at 500 °C for 2 h, purged with Ar, and cooled to room temperature. After H_2 adsorption at room temperature for 1 h, TPD spectra were collected by heating the catalysts at 20 °C/min in Ar. H_2 desorption was measured using a thermal conductivity detector (TCD).

3.2.3. XPS

XPS was used to determine the chemical and electronic nature of the catalyst surface elements. Spectra were collected on a Thermo Escalab 250 spectrometer equipped with an Al anode (Al$K\alpha = 1486.6$ eV). Measurements were carried out with a 20 eV pass energy, a 0.1 eV step, and a 0.1 s dwelling time. The Al 2p peak of Al_2O_3 at 74.3 eV was used as a reference for energy corrections.

XPS was performed for the calcined and reduced catalysts. Catalyst reduction was carried out ex-situ using the following procedure. The temperature was increased from room temperature to 120 °C at 5 °C/min and held at this temperature for 1 h under flowing Ar to remove adsorbed moisture. The catalysts were then heated in pure hydrogen to 750 °C at 5 °C/min and reduced at this temperature for 1 h. After reduction, the catalysts were purged with Ar at 750 °C and cooled to room temperature. Thereafter, the catalysts were kept under an Ar atmosphere and transferred into the XPS sample holder using a glove box with less 0.1 ppm water and O_2. Finally, the XPS samples were transferred into the XPS chamber without exposure to air. The reduction procedure is similar to the reduction procedure followed in the catalytic studies.

XPS spectra were recorded at an angle of 90° for the X-ray source. The atom fraction of each element in the catalyst sample, C_x, was calculated using [20]:

$$C_x = \frac{n_x}{\sum n_i} = \frac{I_x/S_x}{\sum I_i/S_i}, \quad (3)$$

where I_x is the time-normalized intensity of the B 1s, the Al 2p, or the Ni 2p peak, and S_x is the corresponding atomic sensitivity factor for X-ray sources at 90°, i.e. 0.19 for B 1s, 0.22 for Al 2p, 14.61 for Ni $2p_{3/2}$ and 7.57 for Ni $2p_{1/2}$. XPS spectra in Fig. 3 were normalized against I_{Al}.

3.2.4. Scanning electron microscopy (SEM)

The morphology of the catalysts after 450 min on stream was examined on a JEOL Feg SEM (SM 6700F).

3.2.5. Temperature-programmed oxidation (TPO)

To determine the effect of boron promotion on the amount of carbon deposited, TPO was performed on catalyst samples after 450 min on stream under conditions specified below. A 15 mg catalyst sample was placed in a quartz cell, pretreated with Ar (200 °C for 1 h), and oxidized in a 5 vol% O_2/Ar stream, using a linear temperature program of 20 °C/min to 800 °C. The TPO profile was recorded with a Hiden HPR20 mass spectrometer at a vacuum of 10^{-6} Torr or better, calibrated with $CaCO_3$ (Sigma–Aldrich, 99.9%).

3.3. Catalyst activity

To test the effect of boron promotion on the catalyst stability and activity, steam methane reforming was carried out in a fixed-bed micro-reactor. The reactor is a 40 cm stainless steel tube with an internal diameter of 4 mm. To reduce the catalysts, the reactor temperature was increased to the reaction temperature (750 or 800 °C) at 5 °C/min and kept at the reaction temperature for 30 min under a 50 Nml/min H_2 stream. Next, the catalysts were exposed to a $CH_4/H_2O/N_2$ mixture. De-ionized water was introduced by a Shimadzu pump (LC-20 AT) followed by a steam generator, and gas flow rates were controlled by Brooks 5850 mass flow controllers. The outlet gases were analyzed, after water condensation, with an on-line Gas Chromatograph (GC-2010, Shimadzu) equipped with a thermal conductivity detector.

The catalysts were evaluated for three sets of reaction conditions: (1) A reaction temperature of 800 °C, a total pressure of 1 atm, CH_4:H_2O:N_2 ratios of 10:10:1, and a methane flow rate of 50 Nml/min. To reduce mass transfer limitations, 20 mg catalyst (sieved to 212–300 μm) was diluted with 50 mg SiC (with a particle size of 250–400 μm), leading to a total Gas Hourly Space Velocity (GSHV) of 330,000 $cm^3/(h\,g_{cat})$; (2) The GHSV was further increased to 660,000 $cm^3/(h\,g_{cat})$ by reducing the catalyst to 10 mg to test the effect of boron promotion on catalyst stability at higher space velocities and to further reduce possible mass transfer limitations. Other conditions remained unchanged. (3) To prepare the catalysts for TPO analysis, 50 mg undiluted catalyst was used. To reduce mass transfer limitations at this space velocity, the reaction was run at a slightly lower temperature, 750 °C, and for CH_4:H_2O:N_2 ratios of 1:1:1. The methane flow rate of 50 Nml/min corresponds to a GHSV of 180,000 $cm^3/(h\,g_{cat})$. Other reaction conditions remained unchanged.

4. Results and discussion

4.1. Catalyst characterization

The effect of boron on the particle size and the dispersion of the calcined catalysts were examined with XRD. An average particle size of 8–9 nm was determined for NiO. Boron did not have a significant effect on the XRD spectra and on the NiO diameters. Using Eqs. (1) and (2), a dispersion of about 10% was estimated for all three catalysts. The limited effect of boron is to be expected,

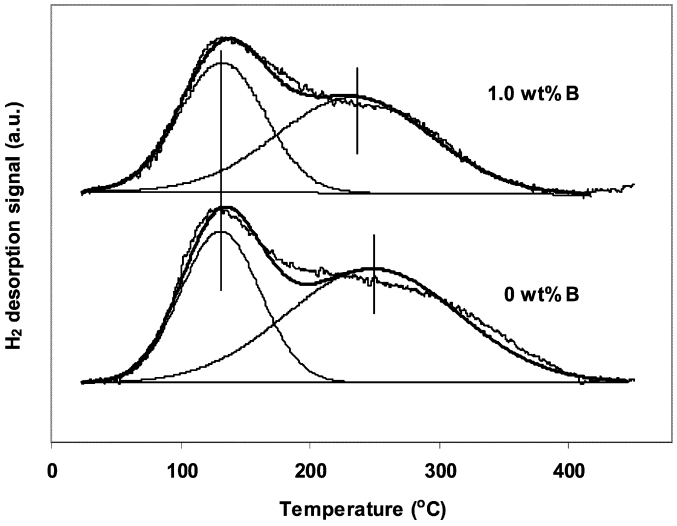

Fig. 2. H_2 TPD profiles for 15 wt% Ni/γ-Al_2O_3 catalysts, unpromoted and promoted with 1.0 wt% B.

Table 2
Bulk composition (ICP-OES), surface composition (XPS), particle size (XRD), H_2 TPD and dispersion for calcined 15 wt% Ni/γ-Al_2O_3 catalysts promoted with boron.

Catalyst	Bulk atomic ratio Ni:B	Surface atomic ratio Ni:B	XRD			H_2 TPD, H_2 uptake ($\mu mol/g_{cat}$)
			d(NiO) (nm)	d(Ni)[a] (nm)	D[b] (%)	
0 wt% B	1:0	1:0	8.7	7.3	10.3	45.0
0.5 wt% B	1:0.18	1:0.64	9.4	7.9	9.6	40.6
1.0 wt% B	1:0.37	1:1.4	8.6	7.2	10.5	37.9

[a] From d(NiO) using Eq. (1).
[b] Eq. (2).

since boron was added to the Ni catalysts after drying and calcination. Based on transmission electron microscopy studies, Chen et al. [21] reported that addition of B to a 1.0 wt% Ni catalyst reduces the size of the Ni particles by serving as the structural promoter. However, Chen et al. used a significantly lower Ni loading.

H_2 TPD was used to probe the active sites. The H_2 TPD profiles for the catalysts with 0.0 and 1.0 wt% B are shown in Fig. 2, and the H_2 uptakes for the different catalysts are given in Table 2. Promotion with 0.5 and 1.0 wt% B decreases the H_2 uptake slightly by 10 and 16%, respectively. Note that complete NiO reduction is difficult [14], and at the TPD reduction temperature, 500 °C, the reduction is not complete. Hence, the variation in the hydrogen uptake might, in part, be attributed to a variation in the degree of reduction at those conditions. The TPD profiles in Fig. 2 show two peaks, a low temperature peak at about 130 °C, and a broader peak between 230 and 250 °C, suggesting the existence of at least two types of adsorption sites. The low temperature peak is relatively unaffected by B promotion, but the high temperature peak shifts down by about 20 °C, and the ratio between the high and the low temperature peak decreases from 1.9 to 1.3. This suggests a decrease in the number and strength of the stronger adsorption sites, possibly caused by partial blocking by B.

The effect of reduction on the chemical state of Ni and B was determined using XPS. The Ni 2p spectra for the calcined catalyst (Fig. 3a) are characteristic of Ni oxide (NiO) [22] and exhibit two spin-orbit peaks, corresponding to Ni $2p_{3/2}$ and Ni $2p_{1/2}$, at binding energies of 856.9 and 874.4 eV, respectively. Both are accompanied by shake-up satellites at approximately 862.7 and 880.6 eV. After reduction, the Ni $2p_{3/2}$ peak shifts to 852.3 eV, while the Ni $2p_{1/2}$ becomes less intense and shifts to 869.6 eV (Fig. 3b). The Ni $2p_{3/2}$ peak can be assigned to metallic nickel (Ni^0) or nickel boride [23,24], indicating that the catalyst did not re-oxidize during transfer to the XPS chamber. The binding energy for the B 1s peak at 192.3 eV for the calcined catalysts is characteristic of boron oxide (Fig. 3c) [25,26]. After reduction, the B 1s peak for the catalyst promoted with the 1 wt% B exhibits a shoulder at lower binding energy, and can be deconvoluted into a peak at 192.3 eV, corresponding to boron oxide, and a new peak at 189.6 eV, corresponding to nickel boride (Fig. 3d) [24]. The relative peak areas indicate that about 20% of the boron oxide is reduced, and interacting with Ni. Hence, XPS clearly shows a partial reduction of the boron oxide.

Next, surface atomic ratios were determined from the Ni and B XPS peak areas for the calcined catalyst (Fig. 3) using Eq. (3) (Table 2). XPS is a surface sensitive technique and accounts for no more than a few atomic distances through the solid. For the catalyst promoted with 0.5 wt% B, the surface Ni:B atomic ratio of 1:0.64, compared to the bulk ratio of 1:0.18, clearly indicates that boron is preferentially located at the surface. This can be expected since a sequential impregnation procedure was used. However, the surface B:Ni ratio is less than 1, and 0.5 wt% boron might not be sufficient to occupy all the octahedral sites in the subsurface layer, as required to effectively stop carbon diffusion to bulk. Based on first principles modeling (summarized in Section 2), boron was proposed to block all the step sites first, and then occupy all the octahedral sites just below the surface [10,11]. To effectively reduce coking, the calculations suggest that the surface B to surface Ni ratio should be at least 1. The atomic ratio between total B and surface Ni can also be estimated from the Ni dispersion in Table 2. For the 15 wt% Ni/γ-Al_2O_3 catalyst promoted with 0.5 wt% B, this leads to a surface Ni:total B ratio of 1:1.72, and 0.5 wt% boron should be sufficient to cover all surface sites, if a monolayer of boron adsorbs exclusively on the Ni particles. However, boron might also adsorb on the γ-Al_2O_3 support. Indeed, Stranick et al. [27] indicate that B interacts strongly with a γ-Al_2O_3 support and aluminum borate ($9Al_2O_3{\cdot}2B_2O_3$) might form when B is added to a γ-Al_2O_3 supported Co catalyst. This is not surprising, considering that B and Al belong to the same group of the periodic table. Since aluminum borate has a reported B 1s binding energy of 192.5 eV [27], it cannot be ruled out based on the XPS data. To further increase the surface B:Ni ratio, the boron loading was increased to 1.0 wt%, and XPS yields an estimated surface Ni:B ratio of 1:1.4.

Hence, the XPS data suggest that only B atoms interacting with Ni particles can be reduced, while a significant amount of boron oxide, probably interacting with the γ-Al_2O_3 support, cannot be reduced. To confirm this idea, γ-Al_2O_3 without Ni was impregnated with 1 wt% B, and subjected to the reduction procedure. No shift in the B 1s XPS peak could be detected.

In order to quantify the effect of boron on the stability and activity of the 15 wt% Ni/γ-Al_2O_3 catalyst, the catalysts were studied under steam methane reforming conditions. In the next section, we discuss the effect of boron on the methane conversion. TPO studies of the catalysts were performed to quantify the effect of boron on the amount of deposited carbon.

4.2. Methane steam reforming

A series of 15 wt% Ni/γ-Al_2O_3 catalysts with B loadings of 0, 0.5 and 1.0 wt% were synthesized and tested in a fixed-bed micro-reactor. Small amounts of catalyst, 20 and 10 mg, diluted with 50 mg SiC, were used to increase the space velocity to 330,000 $cm^3/(h\,g_{cat})$ and 660,000 $cm^3/(h\,g_{cat})$, respectively. Fig. 4 shows the methane conversion as a function of reaction time for promoted and unpromoted catalysts. The initial methane conversions are far from the equilibrium conversion of 89% for the selected reaction conditions [28]. When the space velocity is doubled, the initial conversion decreases from 56 to 31% for the unprompted catalyst. For a first order rate law, as proposed by Wei

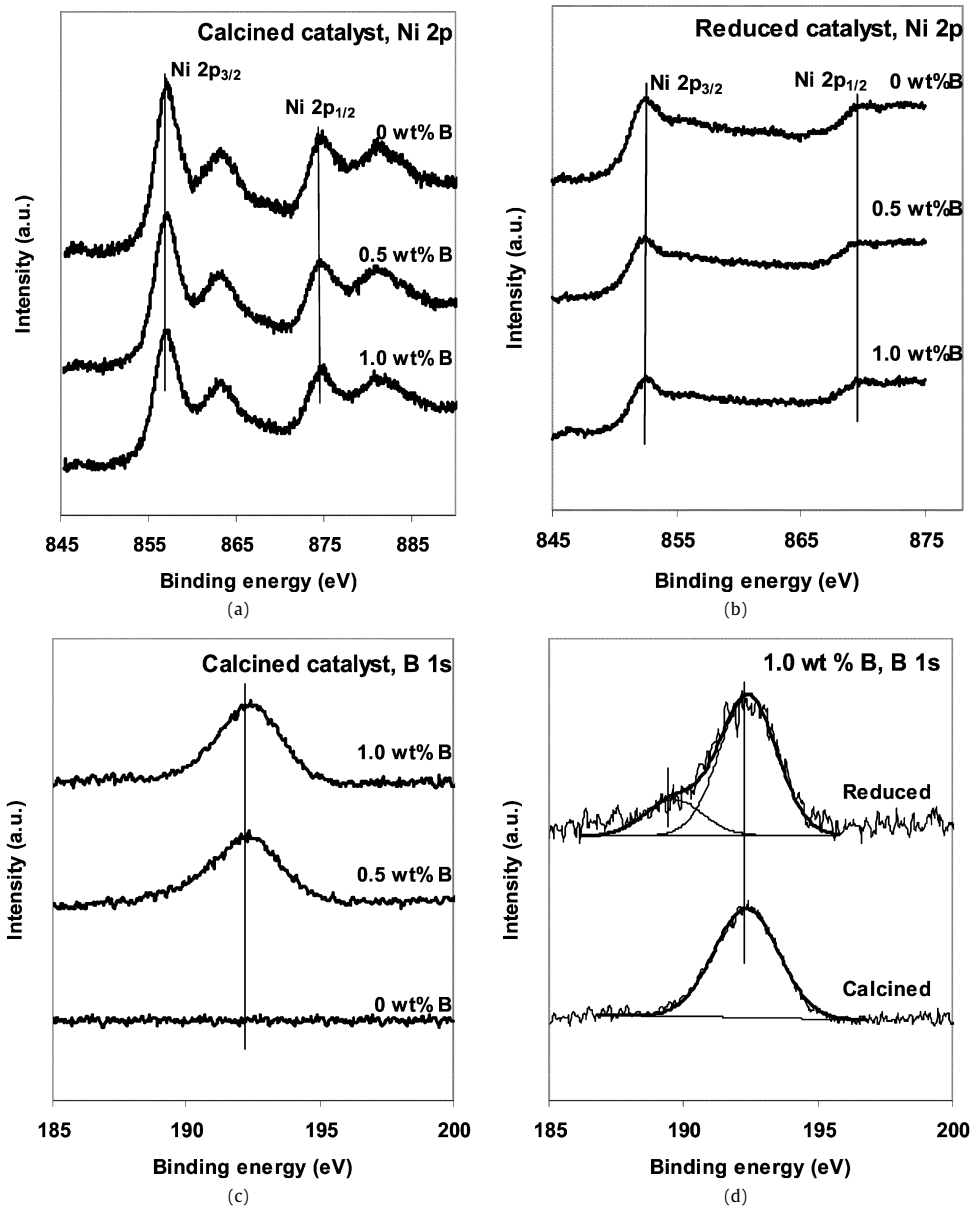

Fig. 3. Ni 2p and B 1s XPS spectra for calcined and reduced 15 wt% Ni/γ-Al_2O_3 catalysts with various amount of boron. The spectra are normalized against Al.

and Iglesia [14], the methane conversion is expected to decrease from 56 to 34% when the space velocity is doubled. The observed decrease hence indicates that the experiments are under kinetic control. Based on the estimated Ni dispersion in Table 2, an average turnover frequency (TOF) over the reactor of 3.8 s^{-1} is obtained. Wei and Iglesia [14] reported a similar TOF of 3.8 s^{-1} for methane steam reforming over a Ni/MgO catalyst. A direct comparison is however difficult, since our experiments were performed at different reaction conditions. Promotion with 1.0 wt% boron increases the initial methane conversion from 56 to 61%. This is consistent with DFT simulations discussed in Section 2 which indicate that subsurface boron atoms do not increase the calculated methane dissociation barrier [11].

To evaluate the effect of boron on the catalyst stability, the methane conversion was normalized against the initial conversion (Figs. 4b and 4d). During the 10 h reaction test, the unpromoted catalyst lost 21% of its initial activity for a GHSV of 330,000 $cm^3/(h\,g_{cat})$ and about 70% of its initial activity for a GHSV of 660,000 $cm^3/(h\,g_{cat})$. Promotion with 0.5 wt% boron did not completely eliminate deactivation, but reduced it from 21 to 14%. Promotion with 1.0 wt% B further reduced the activity loss after 10 h to 6% for a GHSV of 330,000 $cm^3/(h\,g_{cat})$. At a higher GHSV of 660,000 $cm^3/(h\,g_{cat})$, promotion with 1.0 wt% B reduced the activity loss from 70 to 30%. Encouragingly, the residual methane conversion for the promoted catalyst after 10 h is still slightly higher than the initial conversion for the unpromoted catalyst at a GHSV of 330,000 $cm^3/(h\,g_{cat})$ (Fig. 4a). The experiments indicate that promotion with 1.0 wt% B improves the stability and the residual activity of a Ni catalyst, though it does not completely prevent deactivation. DFT calculations [10,11] indicate that B may reduce both nucleation of graphene islands by blocking the step sites, and diffusion of carbon to the Ni bulk. However, graphene may still form on the Ni terraces, especially at high surface carbon concentrations, and step sites might form and disappear spontaneously at the high temperatures during steam reforming [29].

To quantify the deactivation rate, the experimental data were fitted using a first order deactivation model (Figs. 4b and 4d) [30]:

$$-da/dt = ka, \tag{4}$$

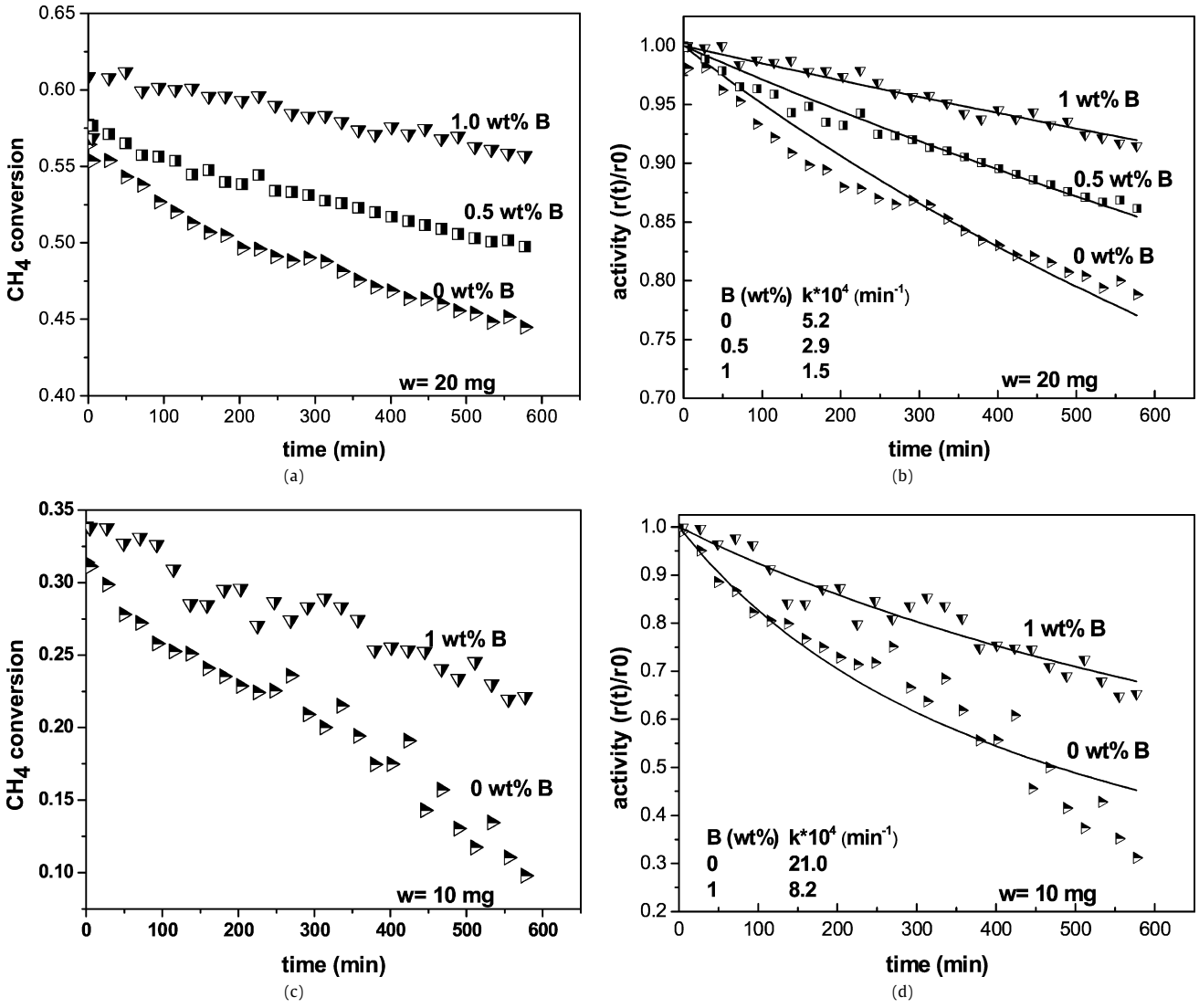

Fig. 4. Methane conversion (a, c) and residual conversion (b, d) as a function of time on stream. Reaction conditions: $T = 800\,^{\circ}C$, $P = 1$ atm, $CH_4{:}H_2O{:}N_2 = 10{:}10{:}1$, methane flow rate = 50 Nml/min, catalyst amount $w = 20$ (a, b) and 10 mg (c, d), and GHSV = 330,000 (a, b) and 660,000 $cm^3/(h\,g_{cat})$ (b, c). Fitted rate coefficients for a first order deactivation model (Eq. (4)) are given in (b) and (d).

where $a(t)$ represents the activity of the catalyst, i.e. relative to the initial rate, and k is the deactivation rate coefficient. For a given catalyst, the deactivation rate coefficient is a function of the operating conditions, namely the temperature and the gas composition. Promotion with 1.0 wt% B decreases the deactivation rate coefficient by a factor of 3 and the promoted catalysts take 3 times longer to lose the same fraction of their initial activity. Increasing the space velocity significantly increases the deactivation rate coefficient. This might be attributed to the higher average methane partial pressure and lower hydrogen partial pressure under those conditions. Note that the deactivation rate in our studies would be too high for industrial applications. This is because reaction conditions were chosen to enhance deactivation. In particular the $H_2O{:}CH_4$ ratio of 1 is much lower than typical industrial values between 4 and 5 [31].

To confirm that the deactivation is caused by carbon deposition, the catalysts were studied by TPO and SEM after the reaction. However, TPO and SEM are less reliable for diluted catalysts, and an additional set of experiments was performed with 50 mg of undiluted catalyst. To reduce mass transfer limitations at the lower GHSV, the reaction temperature was reduced to 750 °C. After

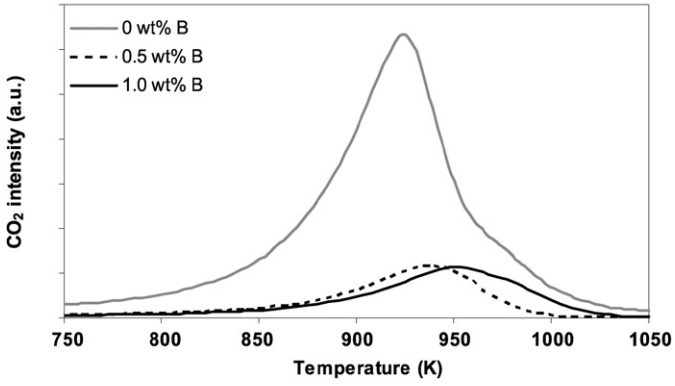

Fig. 5. TPO profiles for 15 wt% Ni/γ-Al_2O_3 with 0.0, 0.5 and 1.0 wt% boron after reaction. Reaction conditions: $T = 750\,^{\circ}C$, $P = 1$ atm, $CH_4{:}H_2O{:}N_2 = 1{:}1{:}1$, methane flowrate = 50 Nml/min, catalyst amount = 50 mg, and GHSV = 180,000 $cm^3/(h\,g_{cat})$. Amount of CO_2 evolved: 1.70 (unpromoted catalyst), 0.31 (0.5 wt% B), and 0.34 $mmol/g_{cat}$ (1.0 wt% B).

450 min on stream, TPO profiles (Fig. 5) and SEM images (Fig. 6) were obtained. Though the activity loss was less than 3% at these conditions for all catalysts, the presence of carbon deposits is il-

(a)

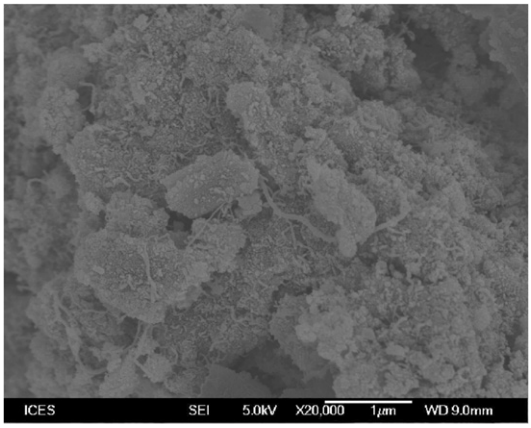

(b)

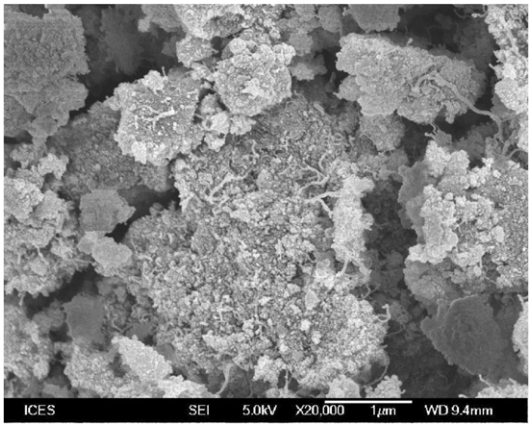

(c)

Fig. 6. SEM images of 15 wt% Ni/γ-Al_2O_3 catalysts after 450 min on stream: (a) unpromoted catalyst; (b) 0.5 wt% B; (c) 1.0 wt% B. Reaction conditions: see Fig. 5.

lustrated by the SEM images and the TPO profiles. Though SEM does not allow quantifying the amount of deposited carbon, it provides qualitative information. After 450 min on stream, the SEM images show significant formation of filamentous carbon on the unpromoted Ni catalysts, while less carbon is observed for the promoted catalysts. The TPO curves indicate that boron reduces the amount of deposited carbon about 5-fold and shifts the TPO curves to slightly higher temperatures. TPO peaks at 925–963 K have been reported earlier, and have been attributed to filamentous carbon [32,33]. The reduction in filamentous carbon deposits by boron promotion is qualitatively confirmed by the SEM images.

5. Conclusions

Theoretical DFT studies indicate that boron and carbon exhibit similar chemisorption preferences on a Ni catalyst and, therefore, boron can be used to selectively block step and subsurface octahedral sites. This is proposed to enhance the stability of Ni catalysts by reducing the nucleation of graphene islands from steps, and by reducing the diffusion of carbon to the subsurface sites and subsequently to the Ni bulk. To validate the theoretical predictions, 15 wt% Ni/γ-Al_2O_3 catalysts, promoted with 0.5 and 1.0 wt% boron were synthesized, characterized and tested during steam methane reforming. The characterization studies indicate that boron might adsorb on both the Ni particles and the γ-Al_2O_3 support, and that 1.0 wt% B should be sufficient to block the step and subsurface sites. Experiments at 800 °C and at a GHSV of 330,000 $cm^3/(h\,g_{cat})$ demonstrate that promotion with 1.0 wt% B not only reduces the first order deactivation rate coefficient by a factor of 3, but also enhances the initial conversion from 56 to 61%. At a higher GHSV of 660,000 $cm^3/(h\,g_{cat})$, 1.0 wt% B reduces the activity loss after 10 h from 70 to 30%. A TPO and SEM study of the catalysts after 450 min of reaction further confirmed that boron assists in preventing carbon buildup.

Acknowledgments

We thank the National University of Singapore and the Science and Engineering Research Council of A*STAR (Agency for Science Technology and Research), Singapore for funding.

References

[1] J.R. Rostrup-Nielsen, in: J.R. Andersson, M. Boudart (Eds.), Catalysis, Science and Technology, vol. 5, Springer, Berlin, 1984, p. 3, chap. 1.
[2] D.L. Trimm, Catal. Today 49 (1999) 3.
[3] J.R. Rostrup-Nielsen, Catal. Today 18 (1993) 305.
[4] J.R. Rostrup-Nielsen, J. Catal. 85 (1984) 31.
[5] N.T. Andersen, F. Topsøe, I. Alstrup, J.R. Rostrup-Nielsen, J. Catal. 104 (1987) 454.
[6] F. Besenbacher, I. Chorkendorff, B.S. Clausen, B. Hammer, A.M. Molenbroek, J.K. Nørskov, I. Stensgaard, Science 279 (1998) 1913.
[7] H.S. Bengaard, J.K. Nørskov, J. Sehested, B.S. Clausen, L.P. Nielsen, A.M. Molenbroek, J.R. Rostrup-Nielsen, J. Catal. 209 (2002) 365.
[8] H.S. Bengaard, I. Alstrup, I. Chorkendorff, S. Ullmann, J.R. Rostrup-Nielsen, J.K. Nørskov, J. Catal. 187 (1999) 238.
[9] E. Nikolla, A. Holewinski, J. Schwank, S. Linic, J. Am. Chem. Sci. 128 (2006) 11354.
[10] J. Xu, M. Saeys, J. Catal. 242 (2006) 217.
[11] J. Xu, M. Saeys, submitted for publication.
[12] O.R. Inderwildi, S.J. Jenkins, D.A. King, J. Am. Chem. Sci. 129 (2007) 1751.
[13] J. Xu, M. Saeys, J. Phys. Chem. C 112 (2008) 9679.
[14] J.M. Wei, E. Iglesia, J. Catal. 224 (2004) 370.
[15] L.P. Nielsen, F. Besenbacher, I. Stensgaard, E. Lægsgaard, C. Engdahl, P. Stoltze, K.W. Jacobsen, J.K. Nørskov, Phys. Rev. Lett. 71 (1993) 754.
[16] Y.H. Chin, D.L. King, H.S. Roh, Y. Wang, S.M. Heald, J. Catal. 244 (2006) 153.
[17] J.L. Lemaitre, P.G. Menon, F. Delannay (Eds.), Characterization of Heterogeneous Catalysts, vol. 15, Dekker, New York, 1984, p. 325.
[18] E.J. Baum, Chemical Property Estimation: Theory and Application, Lewis Publishers, Boca Raton, 1998, p. 3.
[19] M. Boudart, G. Djéga-Mariadassou (Eds.), Kinetics of Heterogeneous Catalytic Reactions, Princeton Univ. Press, Princeton, NJ, 1984, p. 26.
[20] J.F. Moulder, W.F. Stickle, P.E. Sobol, K.D. Bomben, in: J. Chastain, C. King Jr. (Eds.), Handbook of X-Ray Photoelectron Spectroscopy, Physical Electronics, Inc., Eden Prairie, MN, 1995, p. 25.
[21] L. Chen, Y. Lu, Q. Hong, J. Lin, F.M. Dautzenberg, Appl. Catal. A 292 (2005) 295.
[22] S.O. Grim, L.J. Matienzo, W.E. Swartz, J. Am. Chem. Soc. 94 (1972) 5116.
[23] F.U. Hillebrecht, J.C. Fuggle, P.A. Bennett, Z. Zolnierek, Phys. Rev. B 27 (1982) 2179.
[24] J.A. Schreifels, P.C. Maybury, W.E. Swartz, J. Catal. 65 (1980) 195.
[25] A.R. Burke, C.R. Brown, W.C. Bowling, J.E. Glaub, D. Kapsch, C.M. Love, R.B. Whitaker, W.E. Moddeman, Surf. Interface Anal. 11 (1988) 353.
[26] J. Tamaki, H. Takagaki, T. Imanaka, J. Catal. 108 (1987) 256.
[27] M.A. Stranick, M. Houalla, D.M. Hercules, J. Catal. 104 (1987) 396.
[28] M.W. Chase Jr., NIST-JANAF Thermodynamical Tables, in: J. Phys. Chem. Ref. Data, Monograph, vol. 9, fourth ed., 1998, pp. 615, 641, 1310, 1324.

[29] S. Helveg, C. López-Cartes, J. Sehested, P.L. Hansen, B.S. Clausen, J.R. Rostrup-Nielsen, F. Abild-Pedersen, J.K. Nørskov, Nature 427 (2004) 426.
[30] G.F. Froment, K.B. Bischoff (Eds.), Chemical Reactor Analysis and Design, second ed., Wiley, 1990, p. 232.
[31] J.R. Rostrup-Nielsen, J. Sehested, J.K. Nørskov, Adv. Catal. 47 (2002) 65.
[32] M.A. Goula, A.A. Lemonidou, A.M. Efstathiou, J. Catal. 161 (1996) 626.
[33] P. Wang, E. Tanebe, K. Ito, J. Jia, H. Morioka, T. Shishido, K. Takehira, Appl. Catal. A 231 (2002) 35.